Arabidopsis thaliana phytaspase: identification and peculiar properties

DOI:
10.1071/FP16321

Document Version
Accepted author manuscript

Arabidopsis thaliana phytaspase: identification and peculiar properties

Nina V. Chichkova[A], *Raisa A. Galiullina*[A], *Larisa V. Mochalova*[A], *Svetlana V. Trusova*[A], *Zulfazli M. Sobri*[B,C], *Patrick Gallois*[B] *and Andrey B. Vartapetian*[A,D]

[A]Belozersky Institute of Physico-Chemical Biology, Moscow State University, 119 991 Moscow, Russian Federation.

[B]Faculty of Life Sciences, University of Manchester, Oxford Road, Manchester M13 9PT, UK.

[C]Present address: Faculty of Biotechnology and Biomolecular Sciences, Universiti Putra Malaysia.

[D]Corresponding author. Email: varta@genebee.msu.ru

This paper originates from a presentation at the Fourth International Symposium on Plant Signaling and Behavior, *Komarov Botanic Institute RAS*/*Russian Science Foundation*, *Saint Petersburg*, *Russia*, *19–23 June 2016.*

Phytaspases are plant cell death-related proteases of the subtilisin-like protease family that possess an unusual aspartate cleavage specificity. Although phytaspase activity is widespread in plants, phytaspase of *Arabidopsis thaliana* (L.) Heynh. has escaped detection and identification thus far. Here, we show that a single gene (At4 g10540) out of 56 *A. thaliana* subtilisin-like protease genes encodes a phytaspase. The recombinant phytaspase was overproduced in *Nicotiana benthamiana* Domin leaves, isolated, and its substrate specificity and properties were characterised. At pH 5.5, at physiological mildly acidic reaction conditions, the *Arabidopsis* phytaspase was shown to be strictly Asp-specific. The strongly preferred cleavage motifs of the enzyme out of a panel of synthetic peptide substrates were YVAD and IETD, while the VEID-based substrate preferred by the tobacco and rice phytaspases was almost completely resistant to hydrolysis. At neutral pH, however, the *Arabidopsis* phytaspase could hydrolyse peptide substrates after two additional amino acid residues, His and Phe, in addition to Asp. This observation may indicate that the repertoire of *Arabidopsis* phytaspase targets could possibly be regulated by the conditions of the cellular environment. Similar to tobacco and rice phytaspases, the *Arabidopsis* enzyme was shown to accumulate in the apoplast of epidermal leaf cells. However, in stomatal cells *Arabidopsis* phytaspase was observed inside the cells, possibly co-localising with vacuole. Our study thus demonstrates that the *Arabidopsis* phytaspase possesses both important similarities with and distinctions from the already known phytaspases, and is likely to be the most divergent member of the phytaspase family.

Additional keywords: apoplast, aspartate specificity, proteolysis, subtilisin-like protease.

Although plant proteases of the phytaspase family are important contributors to stress-induced plant cell death, phytaspase of a classical model plant *Arabidopsis thaliana* has escaped identification thus far. We identified the *Arabidopsis* phytaspase-encoding gene and characterised the recombinant enzyme. Substrate specificity and

properties of the *Arabidopsis* phytaspase display both important similarities with and distinctions from the already characterised phytaspases.

Introduction

Generally, proteolytic enzymes are poor at hydrolysing peptide bonds after an aspartic acid residue (Asp, D) in their substrates. A notable exception from this tendency is represented by the programmed cell death (PCD)-related proteases, caspases and granzyme B in animals (Talanian *et al*.1997; Thornberry *et al*. 1997) and phytaspases in plants (Chichkova *et al*. 2010, 2012; 2014). Although structurally very different, these endoproteases recognise a short peptide motif in their substrates and introduce a break strictly after an Asp residue. Due to their exceptional selectivity, these proteases hydrolyse a limited number of proteins, usually introducing a single cleavage into their targets. Therefore, these are processing, rather than digestive, proteolytic enzymes.

Plant phytaspases belong to a family of Ser-dependent subtilisin-like proteases (Schaller *et al*. 2012). Prototype members of the phytaspase group, phytaspases from *Nicotiana tabacum* L. (Nt Phyt) and *Oryza sativa* L. (Os Phyt), have been characterised in detail and shown to be essential for the accomplishment of PCD induced by biotic and abiotic stimuli in plants (Chichkova *et al*. 2004, 2010; Fomicheva *et al*. 2012). Transgenic upregulation of phytaspase activity enhanced plant cell death, whereas PCD responses were suppressed in tobacco plants with downregulated phytaspase activity (Chichkova *et al*. 2010).

Phytaspases are synthesised as inactive preproenzymes which are constitutively and autocatalytically processed to generate mature active enzymes that are secreted out of the plant cell into the apoplast (Chichkova *et al*. 2010), which is typical for plant subtilases (Cedzich *et al*. 2009). This constitutive activation explains why phytaspase activity is readily detectable in extracts of control plant tissues (Chichkova *et al*. 2008). PCD-inducing stimuli, such as oxidative and salt stresses or the tobacco mosaic virus-induced hypersensitive response cause phytaspase re-localisation from the apoplast into the stressed plant cell (Chichkova *et al*. 2010; Vartapetian *et al*. 2011).

Nt and Os Phyt share several features. In particular, the preferred cleavage recognition motif for both enzymes estimated with a set of tetrapeptide substrates commonly used to establish caspase/phytaspase cleavage specificity is VEID (Chichkova *et al*. 2010). Recent analysis of the Os Phyt specificity with the use of positional scanning substrate combinatorial peptide libraries revealed, however, that the optimum phytaspase recognition motif is strikingly hydrophobic (Galiullina *et al.* 2015). A single known protein target of phytaspases is the VirD2 protein of a plant pathogenic bacterium *Agrobacterium tumefaciens*. Both Nt and Os Phyt introduce a single break close to the *C*-terminus of VirD2 protein, which resulted in the detachment of the nuclear localisation signal of VirD2 and compromised delivery of the bacterial T-DNA into the plant cell nucleus (Chichkova *et al*. 2004; Reavy *et al*. 2007). Similar VirD2-hydrolysing

activities were documented in extracts of various plant species (Chichkova *et al*. 2008), indicating that phytaspases are ubiquitous in plants. However, the identity of the phytaspase gene in the genome of a classical model plant *Arabidopsis thaliana* (L.) Heynh. escaped identification thus far.

Here we report identification and characterisation of the *A. thaliana* phytaspase (At Phyt). Our study demonstrates that At Phyt possesses both important similarities with and distinctions from the already characterised phytaspases, and is likely to be the most divergent member of the phytaspase family.

Materials and methods

Plasmid construction

The At4 g10540 gene encoding At SBT3.8, a putative subtilisin-like protease, was PCR-amplified and a 3260-bp DNA fragment corresponding to the protein-coding region of the gene was inserted into the pRTL2 vector between the dual 35S promoter and transcription terminator. The whole expression cassette was then transferred into the pLH7000 binary vector. The At SBT3.5 cDNA was obtained by reverse transcription-PCR using total RNA from *Arabidopsis thaliana* (L.) Heynh. (Columbia) as a template, and cloned into the pLH7000 vector similarly. To construct GST and EGFP fusion proteins, the termination codons in subtilase genes were removed, and the tag gene was inserted in frame, downstream of the subtilase gene. Expression cassette with the At SBT3.8-EGFP gene was finally introduced into the pZP111b vector to be used for transient production of the protein in *A. thaliana*.

The S553A mutation was introduced into At4 g10540 gene by QuikChange mutagenesis kit (Stratagene). Sequences of all DNA fragments obtained with the aid of PCR were verified by DNA sequencing.

Production in Nicotiana benthamiana *and purification of recombinant At subtilases*

pLH7000-based expression constructs bearing the subtilase genes were introduced into *Agrobacterium tumefaciens* C58C1 cells. Transformed agrobacteria were infiltrated into *Nicotiana benthamiana* Domin leaves, then 4–5 days post infiltration, leaves were ground in liquid nitrogen, and the samples were suspended in B1 buffer, pH 5.5 (20 mM MES, 2 mM DTT, 0.1% Tween 20, 5% glycerol, 5 0 mM NaCl; 30 mL of the buffer per 10 g of fresh leaves). Debris was eliminated by two successive centrifugation steps, 15 min at 14 000*g* each, and the supernatants were fractionated by ammonium sulfate precipitation. The protein fractions that precipitated within the 50–70% interval of $(NH_4)_2SO_4$ (for untagged At SBT3.8 and GST-tagged At SBT3.5), or within the 40–60% interval (for At SBT3.8-GST) were taken for further purification.

Samples containing GST-fusion proteins were dissolved in PBS buffer, pH 7.3, and dialysed against the same buffer. Proteins were applied onto the glutathione Sepharose resin (GE Healthcare), extensively washed with the same buffer, and the recombinant proteins were eluted from the resin with a PBS buffer, pH 8.0, containing 40 mM glutathione. Western blot analysis of the GST-fused subtilases was performed using anti-GST mouse monoclonal antibody as described (Chichkova *et al*. 2010).

The precipitate containing the untagged At SBT3.8 was dissolved in B1 buffer, pH 6.7, and dialysed against the same buffer. The sample was then applied onto a DE53 column (Whatman) equilibrated with the same buffer and washed with the buffer. Elution was performed with a 0–500 mM NaCl gradient in the same buffer, protein fractions eluted at 30–80 mM NaCl and containing phytaspase activity were collected and dialysed against a PBE buffer (25 mM imidazole, 2 mM DTT, 0.1% Tween 20, 5% glycerol), pH 7.4

The protein sample (0.5 mL) was then subjected to chromatofocusing using a PBE94 Polybuffer Exchanger column (Amersham Biosciences, volume 7 mL) equilibrated with the PBE buffer. The column was washed with the same buffer, and the proteins were eluted from the column with a mixture of 8-fold diluted Polybuffer 74 (70%) and Polybuffer 96 (30%), pH 5.0, containing 2 mM DTT, 0.1% Tween 20, and 5% glycerol. For each fraction of eluate, the pH and phytaspase activity were measured. Protein fraction eluted at pH 6.06 and containing the maximum phytaspase activity was concentrated using YM-30 Centricon (Amicon).

Finally, the untagged At Phyt sample was subjected to non-denaturing polyacrylamide gel electrophoresis using the discontinuous Laemmli system (Laemmli 1970) lacking SDS. Electrophoresis was performed at +4°C until the tracking dye bromophenol blue migrated for 6 cm. The gel was sliced into 2 mm wide bands, proteins were eluted from crushed gel pieces with B1 buffer, pH 6.5, and polyacrylamide gel was discarded by centrifugation. The supernatants were analysed for protein content by SDS-gel electrophoresis and for phytaspase activity.

The protein sample displaying a single protein band and high level of phytaspase activity was subjected to size exclusion chromatography using a Superdex 200 (GE Healthcare) column equilibrated with B1 buffer, pH 6.5, containing 150 mM NaCl, and pre-calibrated with the MW markers. Fractions were processed for phytaspase activity, and protein content was verified by SDS-gel electrophoresis followed by silver nitrate staining.

Detection and quantification of At phytaspase activity

Phytaspase activity of purified enzymes and crude extracts was determined using a panel of synthetic peptide substrates containing a fluorogenic AFC group (from American Peptide Co., Anaspec, Bachem,

Calbiochem, California Peptide, Enzo Life Sciences, MP Biomedicals). Peptide substrates were tested at concentrations of 20–40 µM, as indicated in the figure legends (Chichkova *et al*. 2010). Crude leaf extracts were 5–10-fold diluted before activity measurements. Kinetic measurements of fluorescence intensities were performed in B1 buffer with the indicated pH, containing 0.5 M NaCl at 30°C. Sodium acetate, MES, and HEPES were used at 20 mM to obtain buffers covering pH intervals 4.0–5.0, 5.5–6.5, and 7.0–8.0, respectively. FLUOstar OPTIMA reader (BMG Labtech) equipped with 405 nm excitation and 520 nm emission filters was used to quantitate fluorescence intensities.

Peptide aldehyde inhibitors (Bachem, from stock solution in DMSO) were added, where indicated, to At phytaspase samples up to the concentration of 80 µM. Control samples were supplied with an equivalent amount of DMSO. The mixtures were incubated at 30°C for 30 min before addition of fluorogenic substrates (final concentration 40 µM), and incubation was continued at 30°C for 3 h.

The sensitivity of At phytaspase to various inhibitors of proteolytic enzymes was assessed using an INHIB1 Protease Inhibitor Panel (Sigma) according to recommendations of the manufacturer. At phytaspase was pre-incubated in B1 buffer, pH 6.5, at 30°C for 30 min with the inhibitors at the following concentrations: AEBSF, 1 mM; PMSF, 1 mM; aprotinin, 5 µg mL^{-1}; antipain, 100 µM; leupeptin, 50 µg mL^{-1}; N-ethylmaleimide (NEM), 1 mM; E-64, 10 µM; benzamidine-HCl, 4 mM; trypsin inhibitor, 10 µg mL^{-1}; 6-aminohexanoic acid (6-AHA), 5 mg mL^{-1}; EDTA, 1 mM; phosphoramidon, 10 µM; bestatin, 40 µM; pepstatin A, 1 µg mL^{-1}; chymostatin, 200 µg mL^{-1}; $HgCl_2$, 200 µM. The Ac-YVAD-AFC substrate (20 µM) was then added to the samples, and incubation was continued.

Production and localisation of At phytaspase in A. thaliana

Agro-infiltration for transient expression into *A. thaliana* seedlings was carried out essentially as described in Marion *et al*. (2008) using cut-out nylon mesh with 500 µm pore size (Saatitech, PA500/38) on solidified 3 mL half-strength MS (2.2 g L^{-1} Murashige and Skoog, 10 g L^{-1} glucose, 0.5 g L^{-1} MES, 4 g L^{-1} phytagel, pH 5.7) in a six-well plate with aluminium foil covering the bottom and side of the plate to prevent the cotyledons from growing underneath the mesh. Seedlings were grown for 4 days (22°C, 8 h light/16 h dark cycle) before agro-infiltration. Transformed GV3101-Agrobacterium strain was grown in 2YT (16 g L^{-1} bacto-tryptone, 10 g L^{-1} yeast extract, 5 g L^{-1} NaCl pH7) at 30°C, harvested by centrifugation at 4000*g* for 10 min and resuspended at OD_{600} of 2.0 in the infiltration buffer (5% sucrose, 200 µM acetosyringone). Two mL of resuspended culture was added into each well, covering the seedlings and –1 atm vacuum was applied twice for 1 min. Excess infiltration liquid was completely removed to avoid contamination and the seedlings were grown further for 3 days before confocal analysis. Membranes were labelled with FM4–64 at 1 µM and EGFP-fusion subcellular localisation was monitored

using a Leica SP5 AOBS Tandem Head Confocal using EGFP (ex 488 nm, em 509 nm) and mRFP filters (ex 587 nm, em 610 nm).

Results

Phytaspase activity in A. thaliana *extracts is extremely low*

To detect phytaspase activity in *A. thaliana* plants, extracts were prepared from whole plants or leaves. Incubation of these extracts with canonical fluorogenic peptide substrates of tobacco (*Nicotiana tabacum*) and rice (*Oryza sativa*) phytaspases (Ac-VEID-AFC, Ac-IETD-AFC, Ac-YVAD-AFC, where AFC is 7-amino-4-trifluoromethylcoumarin) (Chichkova *et al*. 2010) has revealed that the presumptive phytaspase activity in *Arabidopsis* is extremely low, compared with extracts from tobacco and rice leaves, Fig. 1*a*. This precluded identification of the preferable substrate of the putative *A. thaliana* phytaspase and, furthermore, hampered purification approaches for isolation and identification of the enzyme.

Predicting the A. thaliana *phytaspase*

To overcome this problem, we took a bioinformatics approach to identify an At Phyt. All known phytaspases belong to a family of subtilisin-like proteases (subtilases), which is represented in *A. thaliana* by 56 members (Rautengarten *et al*. 2005). Plant subtilases are synthesised as preproenzymes encompassing an *N*-terminal signal peptide, an inhibitory prodomain, and a peptidase domain (Chichkova *et al*. 2010; Vartapetian *et al*. 2011), whereas mature active enzymes lack both the signal peptide and the prodomain. Importantly, processing of the enzyme precursor (detachment of the prodomain) was shown to occur autocatalytically in the case of phytaspases and in line with the enzyme aspartate specificity (Chichkova *et al*. 2010). This implies that an aspartate residue (D) should reside at the junction of the prodomain and the peptidase domain. Indeed, such a D residue is located at the very *C*-terminus of the prodomains of tobacco and rice phytaspases, and mutating this D residue is known to preclude processing and activation of phytaspase (Chichkova *et al*. 2010).

We therefore checked whether in any of 56 *A. thaliana* subtilisin-like protease sequences there is an Asp residue at the prodomain-peptidase domain junction. It turned out that a single *A. thaliana* subtilase, SBT3.8, conforms to this pattern (Fig. 1*b*), and therefore represented a candidate for the role of At Phyt. SBT3.8 displays a moderate amino acid identity with the sequences of Nt Phyt and Os Phyt (~33%) and has not been characterised previously.

At SBT3.8 is a phytaspase

To verify whether SBT3.8 might be an *Arabidopsis* Phyt orthologue, we amplified the corresponding gene (At4 g10540) and cloned it into a binary vector under the control of a strong constitutive 35S promoter. Two plasmid constructs were obtained: one encoding SBT3.8 without artificially added

192 sequences, and another one encoding SBT3.8 with a *C*-terminal GST tag enabling detection and
193 purification of the target protein.

194 To further evaluate our prediction that an Asp residue at the *C*-terminus of a subtilase prodomain may
195 serve as an indicator of phytaspase activity, in parallel, we constructed an At SBT3.5-GST fusion protein.
196 At SBT3.5 (774 aa long) displays 77% sequence identity with At SBT3.8 (775 aa long) but lacks an Asp
197 residue at the prodomain-peptidase domain junction (Fig. 1*b*) and was used as a control. *Agrobacteria*
198 transformed with each of the constructs were infiltrated into *N. benthamiana* leaves for transient
199 production of the recombinant proteins. GST-tagged SBT3.8 and SBT3.5 subtilases were isolated from
200 the extracts of infiltrated leaves, affinity purified by glutathione Sepharose chromatography, and
201 displayed a single protein band of the expected size (~110 kDa) when analysed by western blotting using
202 an anti-GST antibody (Fig. 1*c*). A similar electrophoretic mobility was previously reported for processed
203 Nt Phyt-GST fusion protein (Chichkova *et al*. 2010).

204 To assess phytaspase (aspartate) cleavage specificity, the recombinant proteins were incubated with
205 various fluorogenic peptide substrates for caspases and phytaspases with the general structure Ac-XXXD-
206 AFC (X is an amino acid residue). Of the 10 potential substrates tested, SBT3.8 was able to efficiently
207 hydrolyse two: Ac-YVAD-AFC and Ac-IETD-AFC (Fig. 2). In contrast, only background activity was
208 observed with SBT3.5 using any of the substrates (Fig. 2).

209 To further confirm the origin of Asp-hydrolysing activity, we predicted the position of a catalytic Ser
210 residue (Ser^{553}) in SBT3.8 using multiple alignments of subtilisin-like protease sequences and substituted
211 it with Ala. The recombinant SBT3.8 (S553A)-GST fusion protein was overproduced in *N. benthamiana*
212 leaves and isolated, as described above for the wild type enzyme. The ability of SBT3.8 to hydrolyse
213 caspase/phytaspase peptide substrates was abolished by the mutation (see Fig. S1, available as
214 Supplementary Material to this paper).

215 In addition, SBT3.8 lacking the GST tag was produced in *N. benthamiana* and purified by several
216 chromatographic steps and electrophoresis (see 'Materials and methods' for details) (Fig. 1*d*). We note
217 that the untagged enzyme (MW ~80 kDa) displayed a 75-fold higher specific activity towards YVAD-
218 and IETD-based substrates, relatively to the GST-tagged version, under the identical reaction conditions.
219 Nevertheless, the order of preferences for different fluorogenic peptide substrates was virtually the same
220 for tagged and untagged SBT3.8 (data not shown, see Fig. 2).

221 Taken together, the obtained data allowed us to conclude that, in line with our prediction, At SBT3.8 is
222 an *A. thaliana* phytaspase (At Phyt). Notably, YVAD is a strongly preferred recognition motif for At

Phyt, whereas the VEID-based substrate is ineffective (Fig. 2). This is in contrast to Nt Phyt and Os Phyt, both of which preferred the VEID motif (Chichkova *et al*. 2010, 2012; Vartapetian *et al*. 2011).

Under specific conditions, At Phytaspase can hydrolyse non-D substrates

Nt and Os Phytaspases were previously shown to be strictly D-specific (Chichkova *et al*. 2010; Galiullina *et al*. 2015). We therefore assessed the ability of At Phyt to hydrolyse non-D substrates. For this purpose, a collection of 10 fluorogenic peptides with an AFC group attached to the C-terminal amino acid residue other than Asp (Ala, Arg, Glu, Gln, His, Leu, Lys, Phe, Tyr) was used.

At the standard acidic conditions of hydrolysis (pH 5.5), no cleavage of non-D substrates by At Phyt was observed (Fig. 3*a*). However upon pH increase to 6.5, significant cleavage of two non-D substrates, Ac-VEPH-AFC and Suc-AAPF-AFC, was detected (Fig. 3*b*). Such a hydrolysis was observed irrespective of whether GST-tagged or untagged samples of At Phyt were used.

pH dependence of the efficiency of hydrolysis of Ac-YVAD-AFC, Ac-VEPH-AFC, and Suc-AAPF-AFC by At Phyt was then assessed more precisely. Fig. 3*c* shows that an overall acceleration of hydrolysis occurred upon pH increase from 4.5 to 7.5. An ability to cleave non-D substrates became evident at the pH 6.0–8.0 interval, yet being somewhat lower than the Ac-YVAD-AFC hydrolysing activity.

We then re-checked whether the Ac-VEPH-AFC and Suc-AAPF-AFC could be hydrolysed by Nt and Os Phyt under similar conditions, and we found no evidence of cleavage at any pH tested (data not shown, and Galiullina *et al*. 2015). To ascertain whether the non-D hydrolysis was a property of At Phyt, or was caused by impurities in the At Phyt preparations, peptide aldehyde inhibitors Ac-YVAD-CHO and Ac-IETD-CHO cognate to the preferred At Phyt substrates were used. Pre-incubation of the enzyme with these inhibitors abolished hydrolysis of not only the D-specific substrates, but also of non-D substrates (Fig. 3*d*). Importantly, mutation of the predicted catalytic Ser^{553} residue of At Phyt abolished hydrolysis of non-D substrates as well (Fig. S1).Thus, it appears likely that At Phyt is able to hydrolyse some non-D substrates at close to neutral and mildly basic pH.

At Phyt is inhibited by PMSF and chymostatin

Nt and Os phytaspases were previously shown to be surprisingly insensitive to a broad range of chemical inhibitors (Chichkova *et al*. 2004, 2008). We assessed whether any of these inhibitors could interfere with the ability of At Phyt to hydrolyse Ac-YVAD-AFC.As shown in Fig. 4, At Phyt turned out to be insensitive (or very slightly sensitive) to the majority of the inhibitors tested; yet two of them – PMSF and chymostatin – caused complete inactivation of the enzyme. This feature is again in a sharp contrast with the inhibition profile of Nt and Os phytaspases.

At Phyt forms a homodimer in solution

The unusual enzymatic behaviour of At Phyt described above prompted us to address some other properties of the enzyme. Previously, Nt Phyt was described to exist as a monomer in solution (Chichkova *et al*. 2014). For some other plant subtilisin-like proteases, dimerisation was reported (Ottmann *et al*. 2009). We therefore assessed the state of the purified untagged At Phyt in solution using size exclusion chromatography.

It was shown that At Phyt efficiently forms homodimers that elute from the column as a 160 kDa protein (Fig. 5*a*), and that are proteolytically active when assessed with the Ac-YVAD-AFC substrate. When native (untagged) Nt Phyt was analysed under the identical conditions, it eluted from the column as a 70 kDa protein, thus behaving like a typical monomer (Fig. 5*b*). Therefore, in this respect, At Phyt is also distinct from the previously characterised phytaspases.

Localisation of At Phyt

To assess the subcellular localisation of At Phyt in *A. thaliana*, a gene encoding At Phyt-EGFP fusion protein was placed under the control of the 35S promoter, and transiently expressed in 4-day-old seedlings using agroinfiltration. Confocal microscopy of cells at the surface of the cotyledons revealed that At Phyt-EGFP accumulated at the periphery of epidermal cells. Staining cell plasma membranes with FM4–64 dye suggested that the tagged enzyme was located in between the plasma membranes of adjacent cells (Fig. 6*a*). To further strengthen this observation, the agro-infiltrated tissues were plasmolysed with 0.5 M mannitol, 15 min before confocal analysis. This resulted into a mild retraction of the cell protoplasts, and the EGFP fluorescence was clearly visualised in the space between two plasma membranes (red) of the adjacent epidermal cells, corresponding to the apoplast (Fig. 6*b*). We noted that in stomatal cells At Phyt-EGFP fluorescence was observed inside the cells and not in the cell wall (Fig. 6*c*).

Discussion

Up until now, Nt and Os phytaspases, cell death-related subtilisin-like proteases with aspartate specificity, served as prototype members of the phytaspase family. Phytaspases from these plant species display several common features. Although belonging to dicot and monocot plant organisms, respectively, they share 53% amino acid identity, have the same preferred peptide substrate Ac-VEID-AFC, and display apoplastic localisation. Furthermore, the Os Phyt could complement Nt Phyt deficiency and restore stress-induced programmed cell death (Chichkova *et al*. 2010). A proteolytic activity with similar properties was demonstrated to be ubiquitous in a wide range of plant species (Chichkova *et al*. 2008, 2014). However, in the model plant *A. thaliana*, phytaspase escaped identification for several years, mainly due to the fact that phytaspase activity in *A. thaliana* extracts is exceedingly low.

Here, we report the identification and characterisation of At Phyt. To do this, we made use of an observation that, because of the self-processing mechanism of pro-phytaspase into phytaspase, there is a requirement for an Asp residue at the prodomain-peptidase domain junction (Chichkova *et al*. 2010). Scanning of the deduced amino acid sequences of all 56 *A. thaliana* subtilisin-like proteases showed that a single enzyme, At SBT3.8, encoded by the At4 g10540 gene, conformed to this rule. The corresponding recombinant enzyme obtained indeed could efficiently hydrolyse two of the commonly used phytaspase substrates, Ac-YVAD-AFC and Ac-IETD-AFC. Further validation of our approach came from the demonstration that At SBT3.5 subtilase implicated in pectin methylesterase 17 processing (Sénéchal *et al*. 2014), although positioned phylogenetically close to the At Phyt but lacking the characteristic junction Asp residue, failed to display an Asp-specific proteolytic activity.

We have shown, however, that the At Phyt we identified is distinct from the already known phytaspases in several aspects. First, At Phyt displays only 32–33% amino acid identity with the Nt and Os Phyt. Related to this, previously performed phylogenetic comparison of Nt and Os phytaspases with the six distinct subgroups of *A. thaliana* subtilases (Rautengarten *et al*. 2005) placed phytaspases within subgroup 1 (Vartapetian *et al*. 2011) whereas At Phyt (At SBT3.8) belongs to subgroup 3. Furthermore, computer modelling and docking studies of Nt Phyt suggested that His331 of the enzyme is likely involved in the required fitting of the substrate P1 Asp within the phytaspase active site (Vartapetian *et al*. 2011). In the Os Phyt sequence, the relevant position is also occupied by a His residue, whereas the At Phyt bears Gly instead of His.

Second, identification of YVAD as a strongly preferred recognition motif for At Phyt, and virtually no activity of the enzyme towards the VEID-based substrate came as a surprise. Although, similar to what is observed with Nt Phyt and Os Phyt, the three aa motif preceding the D residue clearly affects the hydrolysis efficiency by At Phyt, Nt and Os phytaspases both preferred the VEID motif, YVAD being suboptimal (Chichkova *et al*. 2010). Furthermore, while the Ac-YVAD-AFC substrate was the best one for At Phyt among the substrates tested, no hydrolysis of Ac-VAD-AFC was observed (Fig. 2). This is in contrast to Nt and Os phytaspases, which cleave both of these substrates with comparable efficiencies (Chichkova *et al*. 2010). A likely explanation of this peculiarity of At Phyt is that the *Arabidopsis* enzyme may require a tetrapeptide as a minimal recognition sequence.

Third, At Phyt is present as a dimer in solution, whereas Nt and Os Phyt are monomers (this study and Chichkova *et al*. 2014). Fourth, a remarkable property of Nt and Os Phyt is their complete resistance to a broad range of chemical inhibitors, including those commonly used to inactivate Ser-dependent enzymes (Chichkova *et al*. 2008). At Phyt behaves in a more canonical way, being completely inactivated by

PMSF and chymostatin. Fifth, pH optimum for the Nt and Os Phyt-mediated hydrolysis is mildly acidic (pH 5.5–6.0) (Chichkova *et al*. 2008), whereas At Phyt performs much better at neutral pH (7.0–7.5).

But perhaps the most striking difference between the Nt and Os Phyt and At Phyt is the ability of the latter to cleave, at elevated pH, some synthetic peptide substrates after an amino acid residue other than Asp. While at pH below 6.0 the At Phyt behaves as a strictly D-specific enzyme, at pH 6.0–8.0 it was able to hydrolyse Ac-VEPH-AFC and, to a lesser extent, Ac-AAPF-AFC substrates. Since the hydrolysis of these 'non-D' substrates occurred less efficiently than that of Ac-YVAD-AFC, a possibility existed that the 'non-D' hydrolysis was mediated by a contaminating proteolytic activity and not by the At Phyt itself. This interpretation, however, was shown to be unlikely for several reasons. First, hydrolysis of VEPH- and AAPF-based substrates was observed with different versions of recombinant At Phyt samples, an untagged enzyme and a GST-tagged enzyme, which were purified using two distinct protocols. In particular, the isolation of the At Phyt-GST fusion protein involved an affinity chromatography step. Second, peptide aldehyde phytaspase inhibitors, Ac-YVAD-CHO and Ac-IETD-CHO, were able to neutralise both the D-specific activity (as expected) and the 'non-D' hydrolysing activity. Furthermore, the At Phyt(S553/A) mutant failed to hydrolyse both D-specific and non-D substrates. It is thus likely that both activities belong to the same enzyme. This in turn implies that the repertoire of At Phyt targets may depend on the conditions of the cellular environment.

Similarly to tobacco and rice phytaspases (Chichkova *et al*. 2010), the *Arabidopsis* enzyme was shown to be secreted and accumulated in the apoplast of healthy epidermal leaf cells. However, transiently produced At Phyt was also detected inside the stomatal cells. This opens the interesting possibility that sub-cellular localisation of the At Phyt may vary with the cell type.

Summarising, the At Phyt identified is certainly a phytaspase, yet it appears to be the most atypical among known phytaspases. In this regard, identification of protein substrates of At Phyt and elucidation of its role in *A. thaliana* development and stress responses would be of utmost interest and importance.

Acknowledgements

Parts of this work were supported by Russian Science Foundation grant 16-14-10043 (to ABV), by Russian Foundation for Basic Research Grants 14-04-00232 (to N.V.C.) and 14-04-00256 (to ABV) and by BBSRC grant BB/K009478/1 (to P.G.). The Bioimaging Facility microscopes used in this study were purchased with grants from BBSRC, Wellcome Trust and the University of Manchester Strategic Fund.

References

<jrn>Cedzich A, Huttenlocher F, Kuhn BM, Pfannstiel J, Gabler L, Stintzi A, Schaller A (2009) The protease-associated domain and *C*-terminal extension are required for zymogen processing, sorting within the secretory

pathway, and activity of tomato subtilase 3 (SlSBT3). *Journal of Biological Chemistry* **284**, 14068–14078. doi:10.1074/jbc.M900370200</jrn>

<jrn>Chichkova NV, Kim SH, Titova ES, Kalkum M, Morozov VS, Rubtsov YP, Kalinina NO, Taliansky ME, Vartapetian AB (2004) A plant caspase-like protease activated during the hypersensitive response. *The Plant Cell* **16**, 157–171. doi:10.1105/tpc.017889</jrn>

<jrn>Chichkova NV, Galiullina RA, Taliansky ME, Vartapetian AB (2008) Tissue disruption activates a plant caspase-like protease with TATD cleavage specificity. *Plant Stress* **2**, 89–95.</jrn>

<jrn>Chichkova NV, Shaw J, Galiullina RA, Drury GE, Tuzhikov AI, Kim SH, Kalkum M, Hong TB, Gorshkova EN, Torrance L, Vartapetian AB, Taliansky M (2010) Phytaspase, a relocalisable cell death promoting plant protease with caspase specificity. *EMBO Journal* **29**, 1149–1161. doi:10.1038/emboj.2010.1</jrn>

<jrn>Chichkova NV, Tuzhikov AI, Taliansky M, Vartapetian AB (2012) Plant phytaspases and animal caspases: structurally unrelated death proteases with a common role and specificity. *Physiologia Plantarum* **145**, 77–84. doi:10.1111/j.1399-3054.2011.01560.x</jrn>

<jrn>Chichkova NV, Galiullina RA, Beloshistov RE, Balakireva AV, Vartapetian AB (2014) Phytaspases: aspartate-specific proteases involved in plant cell death. *Russian Journal of Bioorganic Chemistry* **40**, 606–611. doi:10.1134/S1068162014060065</jrn>

<jrn>Fomicheva AS, Tuzhikov AI, Beloshistov RE, Trusova SV, Galiullina RA, Mochalova LV, Chichkova NV, Vartapetian AB (2012) Programmed cell death in plants. *Biochemistry* **77**, 1452–1464. doi:10.1134/S0006297912130044</jrn>

<jrn>Galiullina RA, Kasperkiewicz P, Chichkova NV, Szalek A, Serebryakova MV, Poreba M, Drag M, Vartapetian AB (2015) Substrate specificity and possible heterologous targets of phytaspase, a plant cell death protease. *Journal of Biological Chemistry* **290**, 24806–24815. doi:10.1074/jbc.M115.675819</jrn>

<jrn>Laemmli UK (1970) Cleavage of structural proteins during the assembly of the head of bacteriophage T4. *Nature* **227**, 680–685. doi:10.1038/227680a0</jrn>

<jrn>Marion J, Bach L, Bellec Y, Meyer C, Gissot L, Faure JD (2008) Systematic analysis of protein subcellular localization and interaction using high- throughput transient transformation of *Arabidopsis* seedlings. *The Plant Journal* **56**, 169–179. doi:10.1111/j.1365-313X.2008.03596.x</jrn>

<jrn>Ottmann C, Rose R, Huttenlocher F, Cedzich A, Hauske P, Kaiser M, Huber R, Schaller A (2009) Structural basis for Ca^{2+}-independence and activation by homodimerization of tomato subtilase 3. *Proceedings of the National Academy of Sciences of the United States of America* **106**, 17223–17228. doi:10.1073/pnas.0907587106</jrn>

<jrn>Rautengarten C, Steinhauser D, Büssis D, Stintzi A, Schaller A, Kopka J, Altmann T (2005) Inferring hypotheses on functional relationships of genes: analysis of the *Arabidopsis thaliana* subtilase gene family. *PLoS Computational Biology* **1**, e40. doi:10.1371/journal.pcbi.0010040</jrn>

385 <jrn>Reavy B, Bagirova S, Chichkova NV, Fedoseeva SV, Kim SH, Vartapetian AB, Taliansky ME (2007)
386 Caspase-resistant VirD2 protein provides enhanced gene delivery and expression in plants. *Plant Cell Reports* **26**,
387 1215–1219. doi:10.1007/s00299-007-0335-6</jrn>

388 <jrn>Schaller A, Stintzi A, Graff L (2012) Subtilases – versatile tools for protein turnover, plant development, and
389 interactions with the environment. *Physiologia Plantarum* **145**, 52–66. doi:10.1111/j.1399-
390 3054.2011.01529.x</jrn>

391 <jrn>Sénéchal F, Graff L, Surcouf O, Marcelo P, Rayon C, Bouton S, Mareck A, Mouille G, Stintzi A, Höfte H,
392 Lerouge P, Schaller A, Pelloux J (2014) *Arabidopsis* PECTIN METHYLESTERASE17 is co-expressed with and
393 processed by SBT3.5, a subtilisin-like serine protease. *Annals of Botany* **114**, 1161–1175.
394 doi:10.1093/aob/mcu035</jrn>

395 <jrn>Talanian RV, Quinlan C, Trautz S, Hackett MC, Mankovich JA, Banach D, Ghayur T, Brady KD, Wong WW
396 (1997) Substrate specificities of caspase family proteases. *Journal of Biological Chemistry* **272**, 9677–9682.
397 doi:10.1074/jbc.272.15.9677</jrn>

398 <jrn>Thornberry NA, Rano TA, Peterson EP, Rasper DM, Timkey T, Garcia-Calvo M, Houtzager VM, Nordstrom
399 PA, Roy S, Vaillancourt JP, Chapman KT, Nicholson DW (1997) A combinatorial approach defines specificities
400 of members of the caspase family and granzyme B. Functional relationships established for key mediators of
401 apoptosis. *Journal of Biological Chemistry* **272**, 17907–17911. doi:10.1074/jbc.272.29.17907</jrn>

402 <jrn>Vartapetian AB, Tuzhikov AI, Chichkova NV, Taliansky M, Wolpert TJ (2011) A plant alternative to animal
403 caspases: subtilisin-like proteases. *Cell Death and Differentiation* **18**, 1289–1297. doi:10.1038/cdd.2011.49</jrn>

404 Manuscript received 5 October 2016, accepted 14 December 2016

405 **Fig. 1.** A search for the origin of phytaspase activity in *Arabidopsis thaliana*. (*a*) Comparison of the levels of
406 phytaspase activity in crude leaf extracts of *Nicotiana tabacum*, *Oryza sativa*, and *A. thaliana*. Relative rates of Ac-
407 VEID-AFC, Ac-YVAD-AFC, and Ac-IETD-AFC (40 μM) hydrolysis at pH 5.5 are expressed as a change of
408 relative fluorescence units per hour (ΔRFU h^{-1}, mean values from three experiments, error bars represent s.d.). (*b*)
409 Amino acid sequences of the prodomain-peptidase domain junction in At SBT3.8 and At SBT3.5 subtilases. TTRT
410 or a closely related sequence is located at the very *N*-terminus of the majority of mature plant subtilisin-like
411 proteases. An arrow indicates the site of autocatalytic processing. (*c*) Affinity chromatography purified At SBT3.8-
412 GST and At SBT3.5-GST fusion proteins. Samples were analysed by western blot analysis using anti-GST antibody.
413 Positions of MW markers are shown on the right. (*d*) A sample of untagged At SBT3.8. The protein was fractionated
414 by SDS-gel electrophoresis and stained with Coomassie Blue. Positions of MW protein markers (M) are indicated
415 on the right.

416 **Fig. 2.** At SBT3.8 is an *Arabidopsis* phytaspase. Fluorogenic peptide substrates of caspases and phytaspases (Ac-
417 XXXD-AFC, 40 μM) were incubated with At SBT3.8-GST (black bars) or with At SBT3.5-GST (grey bars) at pH
418 5.5. Data (means from three experiments) are given for approximately equal amounts of both proteins (see Fig. 1*c*).

ΔRFU h^{-1}, relative fluorescence units per hour, error bars represent s.d. An untagged At SBT3.8 displayed the same order of preferences for peptide substrates (data not shown).

Fig. 3. Extended substrate P1 specificity for At Phyt at neutral pH. Peptides (40 μM) used are: Ac-LLY-AFC, Ac-LLL-AFC, Morpholinecarbonyl-HSSKLQ-AFC, Ac-EGR-AFC, Ac-VAE-AFC, Ac-VEIA-AFC, Succinyl-AAPF-AFC, Ac-VEPH-AFC, Ac-TQTE-AFC, D-VLK-AFC. Ac-YVAD-AFC was included as a positive control. Hydrolysis was performed at pH 5.5 (*a*) or pH 6.5 (*b*, *d*). (*c*) pH dependence of Ac-YVAD-AFC, Ac-VEPH-AFC, and Suc-AAPF-AFC hydrolysis by At Phyt. (*d*) Peptide aldehydes Ac-YVAD-CHO and Ac-IETD-CHO abolish hydrolysis of the D-specific substrates (Ac-YVAD-AFC and Ac-IETD-AFC) and of non-D substrates (Ac-VEPH-AFC and Suc-AAPF-AFC). At Phyt was preincubated with the indicated inhibitors (80 μM) or with an equivalent amount of DMSO as a control for 30 min before the addition of the corresponding substrate. Data are given for untagged At Phyt. At Phyt-GST fusion protein behaves similarly (data not shown). ΔRFU h^{-1}, relative fluorescence units per hour. Error bars represent s.d. of triplicates.

Fig. 4. At Phyt is sensitive to PMSF and chymostatin inhibitors. At-Phyt was pre-treated with the indicated chemical inhibitors at the optimised concentration before the addition of the preferred Ac-YVAD-AFC substrate (20 μM). Hydrolysis with untagged At Phyt was performed at pH 6.5. Error bars represent s.d. of triplicates.

Fig. 5. At Phyt forms homodimers in solution. (*a*) A purified untagged At Phyt was subjected to size exclusion chromatography on a Superdex 200 column pre-calibrated with the MW markers: bovine serum albumin (67 kDa), γ-globulin (158 kDa), and thyroglobulin (670 kDa). Phytaspase-containing fractions of the eluate (fractions 32–35) were identified by measuring Ac-YVAD-AFC hydrolysis. Inset: Characterisation of the protein content of the fractions was performed using 15% SDS-gel electrophoresis. The gel was stained with silver nitrate. Abbreviations: IP, input; M, MW protein markers. (*b*) A native (untagged) Nt Phyt was analysed by size exclusion chromatography under the identical conditions. Ac-VEID-AFC was used to identify Nt Phyt-containing fractions. Other procedures and designations were as in (*a*).

Fig. 6. Subcellular localisation of At Phyt fused with EGFP in *Arabidopsis thaliana*. The protein fusion At Phyt-EGFP was transiently expressed in 4-day-old seedlings of *A. thaliana* by agro-infiltration. After 3 days expression and staining in red of the plasma membrane with 1 μM FM4–64, cells on the cotyledon surface were imaged using a confocal microscope. Green channel: EGFP filter, and red channel: mRFP filters for FM4–64. Scale bars = 5 μm. (*a*) Epidermal cells; (*b*) mildly plasmolysed cells using 0.5 M mannitol, 15 min; the space in between the plasma membranes of adjacent cells is enlarged by the protoplast retraction; and (*c*) stomata.

Suppl. Fig. 1. The Ser553Ala mutation in At Phyt abolishes the proteolytic activity of the enzyme. Hydrolysis of Ac-YVAD-AFC, Ac-VEPH-AFC, and Suc-AAPF-AFC substrates (20 μM) with equivalent amounts of the wild type At Phyt-GST (WT, black bars), or with the At Phyt (Ser553Ala)-GST mutant (S553A, grey bars) in a pH 6.5 buffer. ΔRFU/h, relative fluorescence units per hour.

Figure 1.

a).

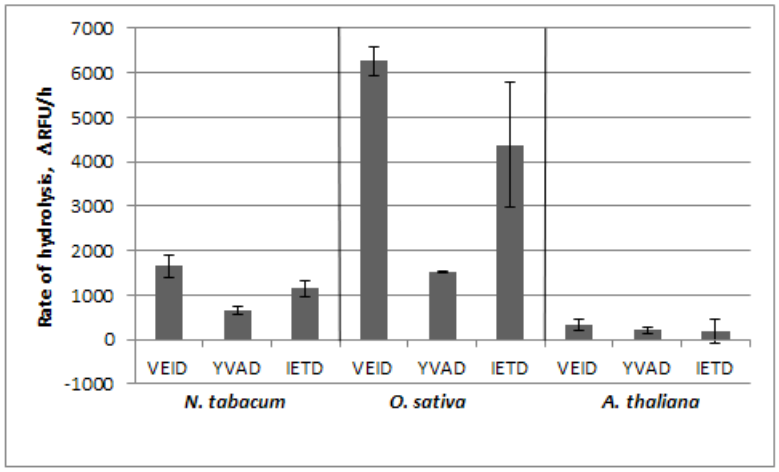

b).

prodomain ↓ peptidase domain

SBT3.8 ...YQLD^{109} TTRT...

SBT3.5 ...YELA^{108} TTRT...

c).

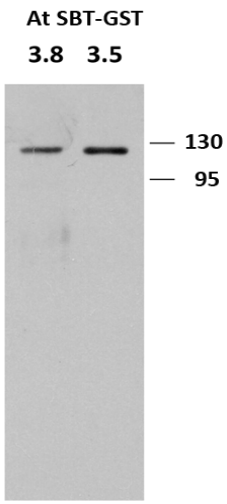

d).

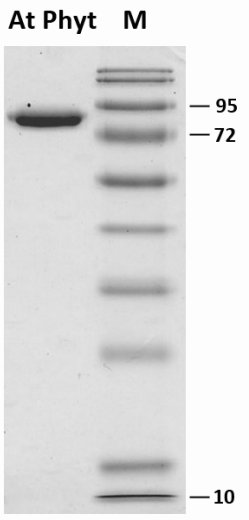

Figure 2.

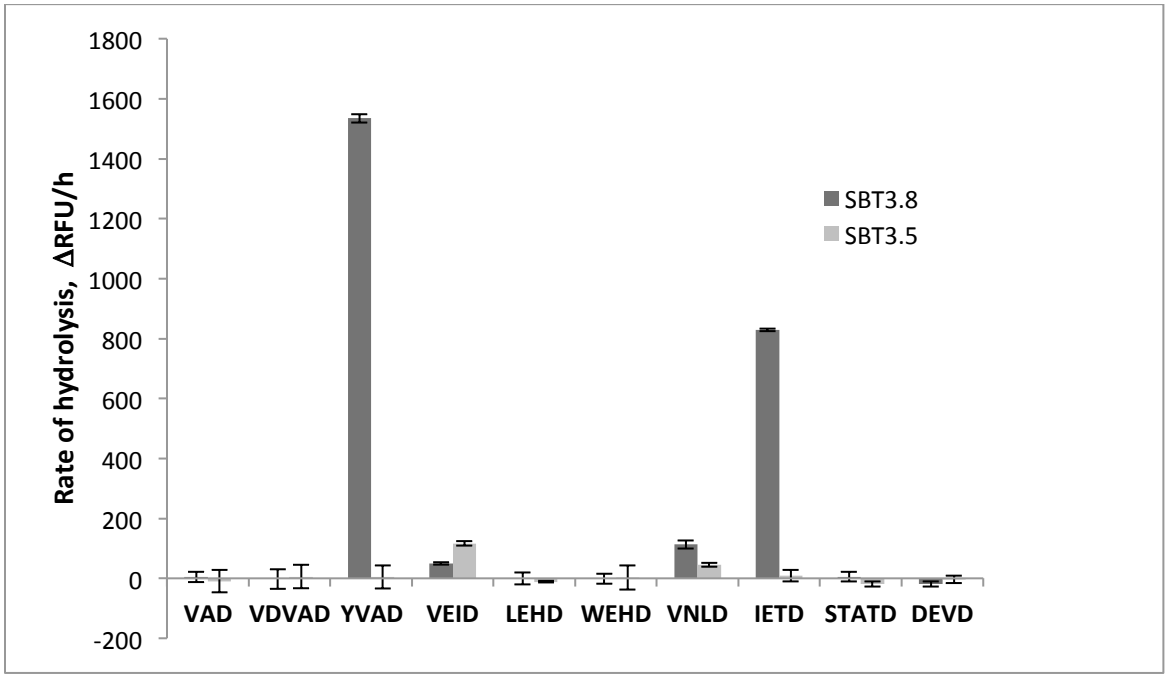
1800
1600
1400
1200
1000
800
600
400
200
0
-200
Rate of hydrolysis, ΔRFU/h
SBT3.8
SBT3.5
VAD
VDVAD
YVAD
VEID
LEHD
WEHD
VNLD
IETD
STATD
DEVD

Figure 3.

a).

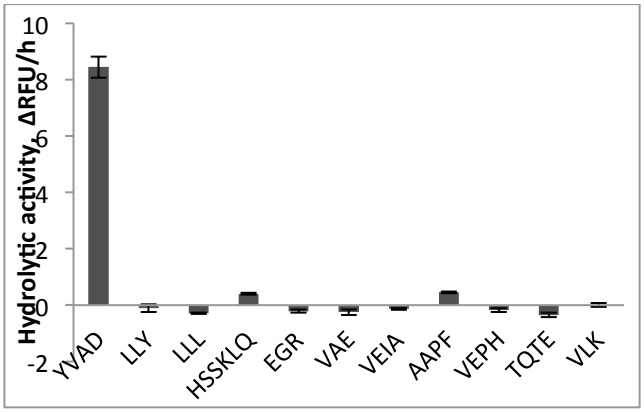
Hydrolytic activity, ΔRFU/h
10
8
6
4
2
0
-2
YVAD
LLY
LLL
HSSKLQ
EGR
VAE
VEIA
AAPF
VEPH
TQTE
VLK

b).

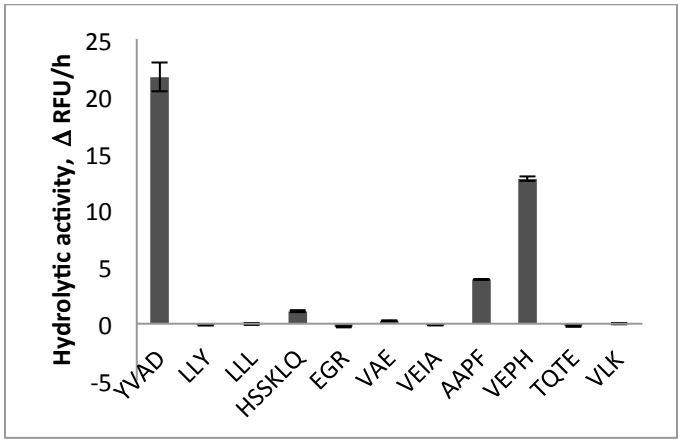
Hydrolytic activity, Δ RFU/h
25
20
15
10
5
0
-5
YVAD
LLY
LLL
HSSKLQ
EGR
VAE
VEIA
AAPF
VEPH
TQTE
VLK

c).

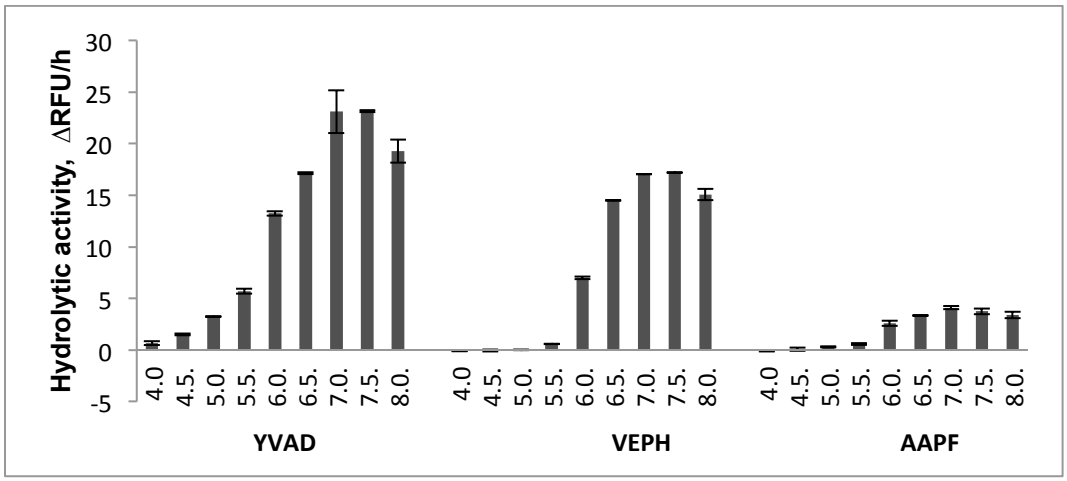
Hydrolytic activity, ΔRFU/h
30
25
20
15
10
5
0
-5
4.0
4.5.
5.0.
5.5.
6.0.
6.5.
7.0.
7.5.
8.0.
YVAD
VEPH
AAPF

d).

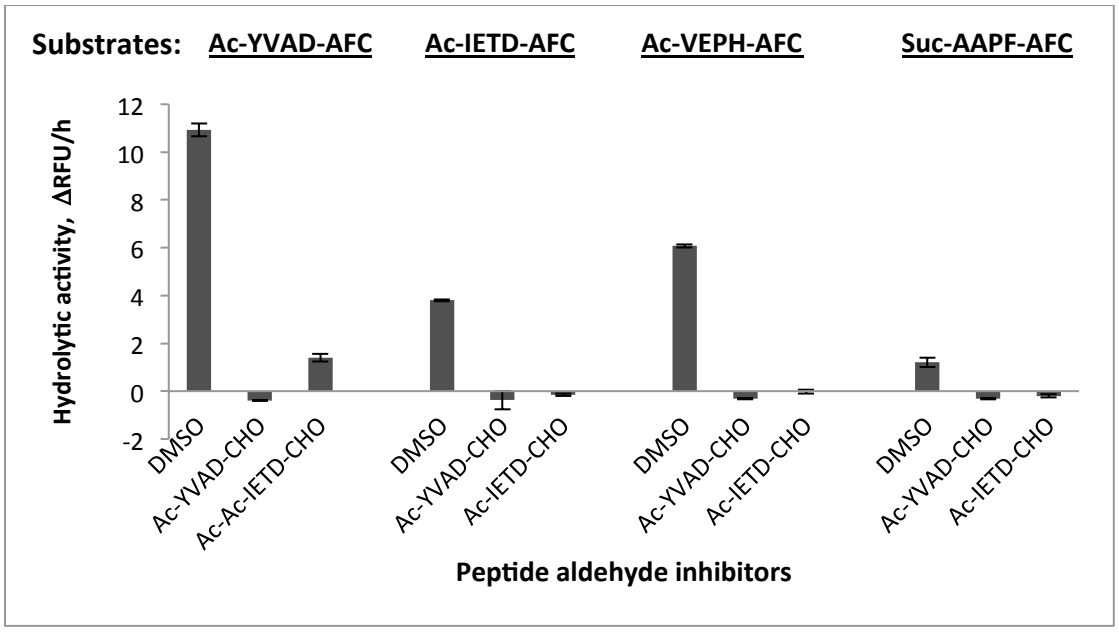
Substrates: Ac-YVAD-AFC Ac-IETD-AFC Ac-VEPH-AFC Suc-AAPF-AFC
Hydrolytic activity, ΔRFU/h
12
10
8
6
4
2
0
-2
DMSO
Ac-YVAD-CHO
Ac-Ac-IETD-CHO
DMSO
Ac-YVAD-CHO
Ac-IETD-CHO
DMSO
Ac-YVAD-CHO
Ac-IETD-CHO
DMSO
Ac-YVAD-CHO
Ac-IETD-CHO
Peptide aldehyde inhibitors

Figure 4.

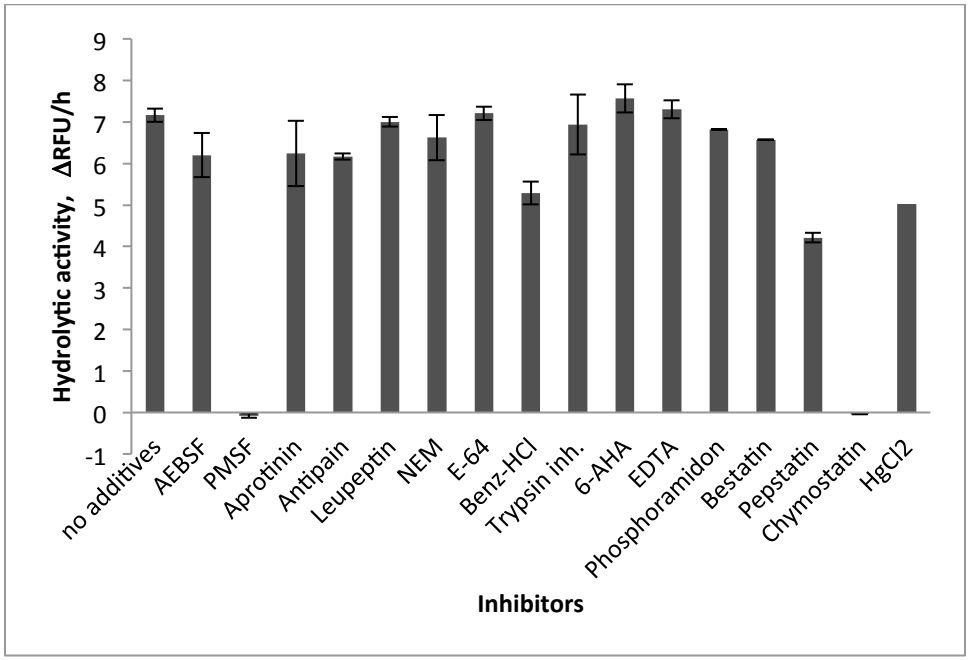
Hydrolytic activity, ΔRFU/h
9
8
7
6
5
4
3
2
1
0
-1
no additives
AEBSF
PMSF
Aprotinin
Antipain
Leupeptin
NEM
E-64
Benz-HCl
Trypsin inh.
6-AHA
EDTA
Phosphoramidon
Bestatin
Pepstatin
Chymostatin
HgCl2
Inhibitors

Figure 5.

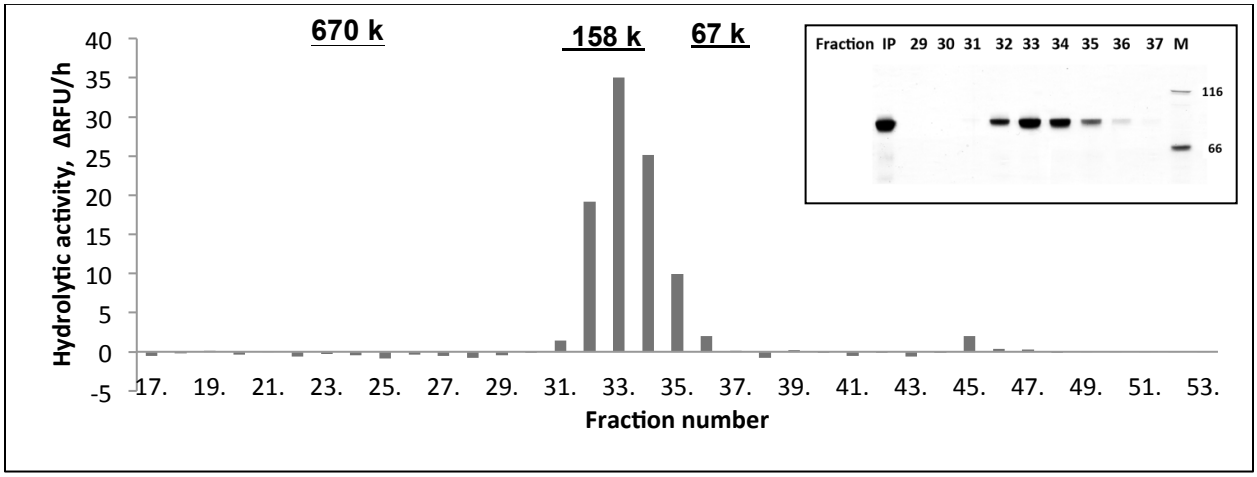

Figure 6.

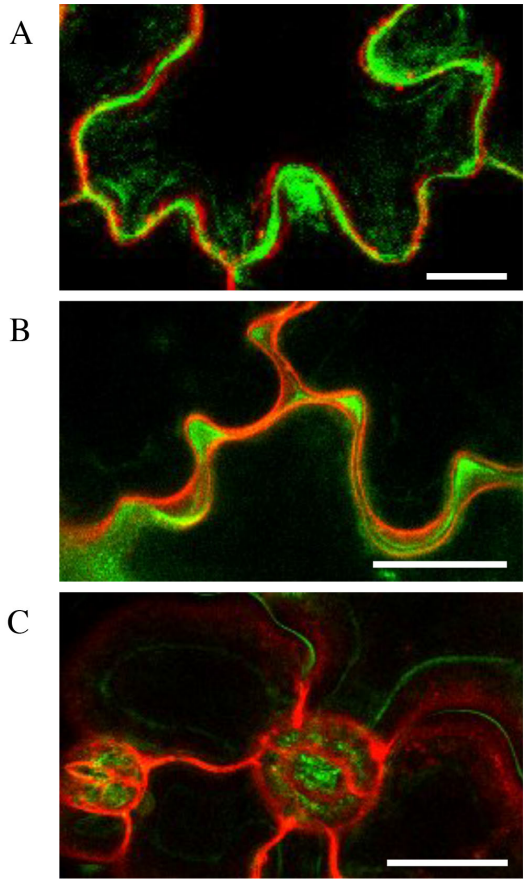

Suppl. Fig. 1.

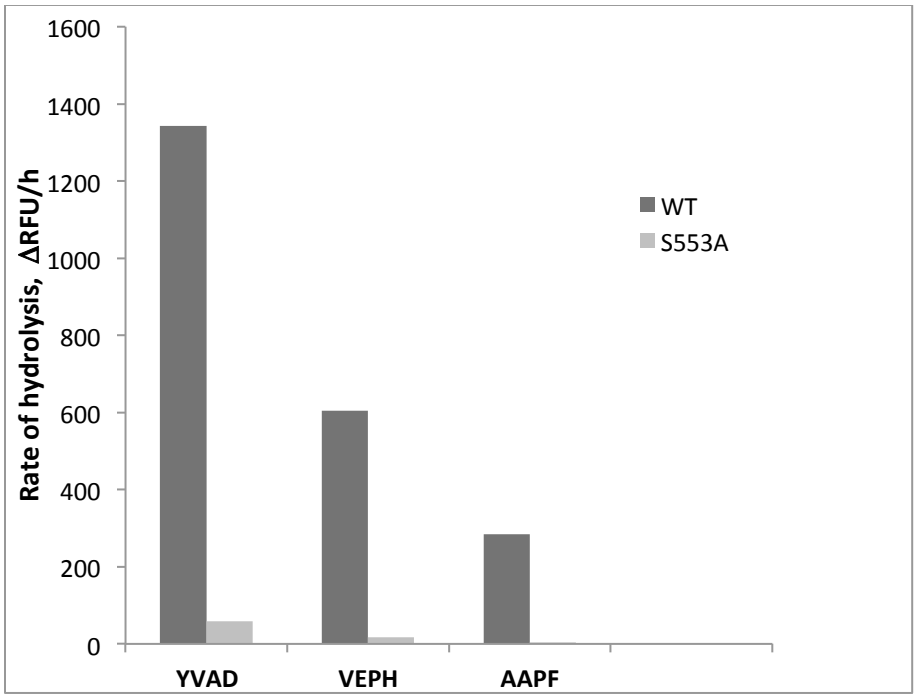
1600
1400
1200
1000
800
600
400
200
0
Rate of hydrolysis, ΔRFU/h
WT
S553A
YVAD
VEPH
AAPF